Growth of $LaAlO_3$ on silicon via an ultrathin $SrTiO_3$ buffer layer by molecular-beam epitaxy

Zhe Wang, Zhen Chen, Antonio B. Mei, Xue Bai, Lena F. Kourkoutis, David A. Muller, and Darrell G. Schlom

Citation: Journal of Vacuum Science & Technology A: Vacuum, Surfaces, and Films **36**, 021507 (2018);
View online: https://doi.org/10.1116/1.5009185
View Table of Contents: http://avs.scitation.org/toc/jva/36/2
Published by the American Vacuum Society

Growth of $LaAlO_3$ on silicon via an ultrathin $SrTiO_3$ buffer layer by molecular-beam epitaxy

Zhe Wang and Zhen Chen
School of Applied and Engineering Physics, Cornell University, Ithaca, New York 14853

Antonio B. Mei
Department of Materials Science and Engineering, Cornell University, Ithaca, New York 14853

Xue Bai
School of Applied and Engineering Physics, Cornell University, Ithaca, New York 14853

Lena F. Kourkoutis and David A. Muller
School of Applied and Engineering Physics, Cornell University, Ithaca, New York 14853 and Kavli Institute at Cornell for Nanoscale Science, Ithaca, New York 14853

Darrell G. Schlom[a)]
Department of Materials Science and Engineering, Cornell University, Ithaca, New York 14853 and Kavli Institute at Cornell for Nanoscale Science, Ithaca, New York 14853

(Received 13 October 2017; accepted 27 November 2017; published 19 December 2017)

(001)-oriented $LaAlO_3$ films were grown epitaxially on (001) Si substrates utilizing an ultrathin 5 unit-cell-thick $SrTiO_3$ buffer layer. The $SrTiO_3$ layer was grown at ~250 °C and annealed in vacuum at 550 °C, following an epitaxy-by-periodic-annealing procedure. Upon this buffer layer, the $LaAlO_3$ layer was then grown by codeposition at 580 °C. The rocking curve of the as-grown $LaAlO_3$ film exhibits a full width at half maximum value as small as 0.02°. Atomic force microscopy shows that the surface of the $LaAlO_3$ film has a root-mean-square roughness of 1.3 Å. Scanning transmission electron microscopy reveals that the $LaAlO_3/SrTiO_3$ interface and the $SrTiO_3$/Si interfaces are sharp. This high crystalline quality, twin-free, epitaxial $LaAlO_3$ on $SrTiO_3$ on silicon could be relevant to integrating oxides with multiple functionalities on silicon. *Published by the AVS.* https://doi.org/10.1116/1.5009185

I. INTRODUCTION

$LaAlO_3$ has a pseudocubic lattice parameter of 3.790 Å,[1] close to that of (001) Si with a 45° in-plane rotation (5.431 Å/$\sqrt{2}$ = 3.840 Å). This close lattice match in combination with thermodynamic stability[2,3] motivates the epitaxial integration of (001) $LaAlO_3$ thin films on (001) Si substrates so that a wide range of functional oxides can be integrated in high quality form with this mainstream semiconductor platform and workhorse. Following its initial use as a low dielectric loss substrate for growing high temperature superconductor thin films such as $ErBa_2Cu_3O_7$,[4] single-crystal (001) $LaAlO_3$ has been a popular substrate for the growth of various epitaxial oxides, ranging from metallic oxides for bottom electrodes including $CaRuO_3$,[5] $La_{1/2}Sr_{1/2}CoO_3$,[6] and $LaNiO_3$;[7] multiferroics like $BiFeO_3$;[8] colossal magnetoresistance materials like $La_{2/3}Ca_{1/3}MnO_3$;[9] metal-insulator transition materials including $NdNiO_3$,[10] photocatalytic materials like the anatase polymorph of TiO_2;[11] tunable dielectrics like $SrTiO_3$ (Ref. 12) and $Ba_xSr_{1-x}TiO_3$;[13] and oxide superlattices with emergent interface ferromagnetism.[14] Therefore, $LaAlO_3$ of high crystalline quality on silicon would pave the way for integrating a plethora of functional oxides with mainstream semiconductor technology.

Historically, $LaAlO_3$ has been grown on silicon using various methods, including metal organic chemical vapor deposition,[15] pulsed layer deposition,[16] sputtering,[17] and atomic layer deposition.[18] Such $LaAlO_3$ films grown directly on silicon are amorphous or polycrystalline, making them unsuitable for the overgrowth of epitaxial functional oxides. Although the $LaAlO_3$/Si interface was shown to be thermodynamically stable[2,3] and the epitaxial growth of both (001) Si on (001) $LaAlO_3$ (Ref. 19) and (111) Si on (111) $LaAlO_3$ (Ref. 20) has been demonstrated, the reverse case—the growth of epitaxial $LaAlO_3$ directly on silicon—has never been achieved. To enable the epitaxial growth of $LaAlO_3$ on silicon, an epitaxial buffer layer that can be directly grown on silicon is introduced. Up to now, the most widely used buffer layer is $SrTiO_3$ grown by molecular-beam epitaxy (MBE).[21–25] With $SrTiO_3$ as the buffer layer, epitaxial $LaAlO_3$ is possible on silicon; however, the crystalline quality of the $LaAlO_3$ layer is far from perfect. Its quality is limited by both the perfection of the $SrTiO_3$ buffer layer and the growth conditions used to prepare the $LaAlO_3$ layer, as evidenced by relatively broad rocking curves from four-circle x-ray diffraction (XRD) measurements.[22,24] By enhancing the crystalline quality of the $LaAlO_3$ layer on top of silicon, we foresee an improvement in the properties of the oxide films that can be epitaxially integrated with silicon. This is because the quality of the materials grown on top of $LaAlO_3$ is restricted by the quality of the $LaAlO_3$ layer underneath.

In this study, we report the growth of $LaAlO_3$ with improved crystalline quality on (001) Si with a 5 unit-cell-thick $SrTiO_3$ buffer layer. After describing the growth conditions in detail, we characterize the resulting improved film

[a)]Electronic mail: schlom@cornell.edu

by XRD, scanning transmission electron microscopy (STEM), and atomic force microscopy (AFM). Many films were grown to perfect the method described in this paper. All the results shown are from the growth of one film—the best one.

II. EXPERIMENT

Both $LaAlO_3$ and $SrTiO_3$ films were grown via MBE in a Veeco GEN10 system with a background pressure in the high 10^{-9} Torr range. Strontium, lanthanum, and aluminum molecular beams were generated with conventional effusion cells from elemental sources, while the titanium beam was generated with a Ti-Ball.[26] Molecular oxygen was introduced and controlled via a piezoelectric leak valve. The substrate temperature was monitored with a thermocouple (that is unfortunately not in direct contact with the sample or sample holder) for temperatures below 500 °C and with an optical pyrometer for temperatures higher than 500 °C. Reflection high-energy electron diffraction (RHEED) was used for *in situ* monitoring of the growth. After sample growth, *ex situ* XRD involving θ-2θ, rocking curves (ω scans), and ϕ scans were made to assess the crystalline perfection of the films. AFM was used to evaluate the surface roughness of the films. The interface abruptness of the heterostructure and its microstructure was investigated using STEM.

The (001) Si substrates (3 in. diameter, *p*-type, boron doped, single-side polished, and resistivity of 0.016–0.017 Ω cm) were cleaned in a commercial ultraviolet ozone cleaner for 20 min to remove organic contamination before being loaded into the MBE chamber. After the native SiO_2 was removed by heating in vacuum to 980 °C for about 20 min, the substrate was cooled down to 600 °C for the deposition of a half of a monolayer of strontium to form a silicide layer for the $SrTiO_3$ growth.[27] Following the epitaxy-by-periodic-annealing process,[28] a 2.5 unit-cell-thick $SrTiO_3$ layer was grown by codeposition at ~250 °C under a low oxygen partial pressure of $(1-3)\times10^{-8}$ Torr. The as-grown 2.5 unit-cell-thick $SrTiO_3$ layer was then annealed at ~550 °C in vacuum to improve its crystalline quality. This process was repeated twice to achieve a 5 unit-cell-thick $SrTiO_3$ buffer layer. More details of the growth of this $SrTiO_3$ buffer layer on silicon are given elsewhere.[28–30]

A 10 nm thick $LaAlO_3$ layer was grown by codeposition on top of the 5 unit-cell-thick $SrTiO_3$ buffer layer on (001) Si in the same growth chamber without breaking vacuum. Prior to the growth of the 10 nm thick $LaAlO_3$ layer, the fluxes of lanthanum and aluminum were calibrated by growing homoepitaxial $LaAlO_3$ on a single-crystal (001) $LaAlO_3$ substrate at 700 °C by codeposition and monitoring the characteristic surface reconstructions using *in situ* RHEED for feedback.[31] If homoepitaxial $LaAlO_3$ is nonstoichiometric and has a lanthanum-rich surface, half-order streaks along the [110] azimuth (pseudocubic notation is used for $LaAlO_3$ throughout this paper) would appear in the RHEED pattern; a slightly aluminum-rich surface would lead to a RHEED pattern with half-order streaks along the [100] azimuth. Based on these surface reconstructions, the temperatures of the lanthanum and aluminum sources were carefully adjusted to provide precisely matched lanthanum and aluminum fluxes. More details of this calibration method are given in Ref. 31. With the closely matched lanthanum and aluminum fluxes, RHEED intensity oscillations of the 01 streak (or the specular spot) were recorded with the RHEED beam incident along the [110] azimuth for homoepitaxial $LaAlO_3$ codeposited at a substrate temperature of 700 °C. The result is shown in Fig. 1. The growth rate of $LaAlO_3$ by codeposition was typically 1 unit cell per minute (23 nm/h).

The growth of a $LaAlO_3$ layer with high crystalline quality on 5 unit cells of $SrTiO_3$ on silicon not only requires well matched (1:1) lanthanum and aluminum fluxes, but also needs a meticulously controlled transitional between the thin $SrTiO_3$, which was grown at relatively low temperature, and the $LaAlO_3$, which was grown at relatively high temperature. This is because 5 unit cells of $SrTiO_3$ (the reason we grew 5 unit cells of $SrTiO_3$ is given in Sec. III) are much thinner than the thickness of the $SrTiO_3$ buffer layers in most epitaxial perovskite oxide thin films grown on $SrTiO_3$ on silicon.[32] Should the 5 unit-cell-thick $SrTiO_3$ on silicon be exposed to oxygen at high temperatures (>500 °C) for a considerable amount of time, the crystalline quality of the thin $SrTiO_3$ buffer layer and the interface between the $SrTiO_3$ and the silicon substrate will be significantly degraded, making it difficult to grow an epitaxial $LaAlO_3$ layer on top. To minimize the exposure of the 5 unit-cell-thick $SrTiO_3$ on silicon to oxygen at high temperatures during the heating-up stage, we started slowly introducing oxygen into the chamber when the $SrTiO_3$-buffered silicon was heated to beyond ~350 °C. In addition, we opened the lanthanum and aluminum shutters simultaneously at 400–450 °C to initiate the growth of $LaAlO_3$. The chamber pressure and the substrate temperature as functions of time were recorded during this transitional stage and are shown in Fig. 2. Soon after the lanthanum and aluminum shutters were opened, the substrate temperature and the oxygen partial pressure reached 580 °C (pyrometer

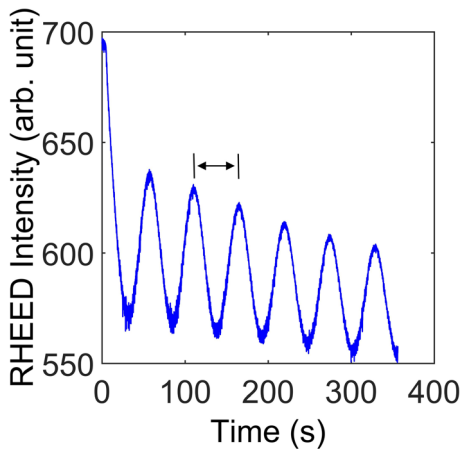

FIG. 1. (Color online) RHEED intensity of the 01 diffraction streak as a function of time showing the growth rate of $LaAlO_3$ by codeposition. The period of the RHEED oscillation marked by the arrow indicates the time needed for the growth of a single unit cell thickness of $LaAlO_3$ along the [001] direction by codeposition. For this work, the growth rate was typically 1 unit cell per minute.

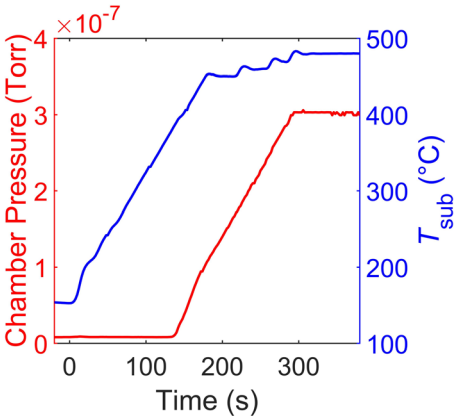

FIG. 2. (Color online) Substrate temperature (T_{sub}) read by the thermocouple and the chamber pressure read by an ion gauge as a function of time during heating of the 5 unit-cell-thick $SrTiO_3$ on silicon for the initiation of the $LaAlO_3$ layer. Oxygen was slowly introduced into the chamber while the substrate was heated. At 400–450 °C, the lanthanum and aluminum shutters were opened simultaneously initiating the $LaAlO_3$ codeposition, before the chamber pressure reached $\sim 3 \times 10^{-7}$ Torr (corresponding to an oxygen partial pressure of $\sim 3 \times 10^{-7}$ Torr).

reading) and $\sim 3 \times 10^{-7}$ Torr, respectively. A 10 nm thick $LaAlO_3$ layer was grown at the elevated temperature of 580 °C under a background oxygen partial pressure of 3×10^{-7} Torr. Although the growth temperature of the $LaAlO_3$ layer is lower than most reports of epitaxial $LaAlO_3$ on $SrTiO_3$ on silicon in the literature,[22,23,33] the films show better crystalline quality, as is shown in Sec. III.

III. RESULTS AND DISCUSSION

We chose 5 unit cells as the thickness of the $SrTiO_3$ buffer layer for the heterostructure [10 nm $LaAlO_3$ on 5 unit cells (2 nm) of $SrTiO_3$ on (001) Si] with both strain and film homogeneity in mind. In terms of the epitaxial strain, $LaAlO_3$ is better lattice matched to (001) Si (1.3% compressive strain) than it is to $SrTiO_3$ (3% compressive strain). Thus, $SrTiO_3$ coherently grown on silicon would be preferred for the growth of a $LaAlO_3$ overlayer compared to the growth of $LaAlO_3$ on a relaxed $SrTiO_3$ layer on silicon. It has been shown that $SrTiO_3$ films above 5 unit cells (2 nm) are partially relaxed on (001) Si.[29,34] Therefore, an $SrTiO_3$ buffer layer with a thickness equal to or below 5 unit cells is optimal for coherent $SrTiO_3$ growth on (001) Si. From the homogeneity perspective, previous work utilizing plan-view STEM showed that there is a phase-separation instability for 2.5 unit-cell-thick $SrTiO_3$ films on (001) Si, resulting in inhomogeneous coverage on (001) Si by $SrTiO_3$ islands.[35] Thus, an $SrTiO_3$ layer thicker than 2.5 unit cells is desired for homogeneous coverage of the underlying silicon substrate. Taking both considerations into account, we grew a 5 unit-cell-thick $SrTiO_3$ buffer layer to make it both coherently strained to the silicon substrate and a reasonably homogeneous buffer layer for the growth of the overlying $LaAlO_3$ film.

In situ RHEED was used to monitor the growth of both the $SrTiO_3$ and the $LaAlO_3$ layers. The RHEED patterns of the 5 unit-cell-thick $SrTiO_3$ buffer layer after growth with

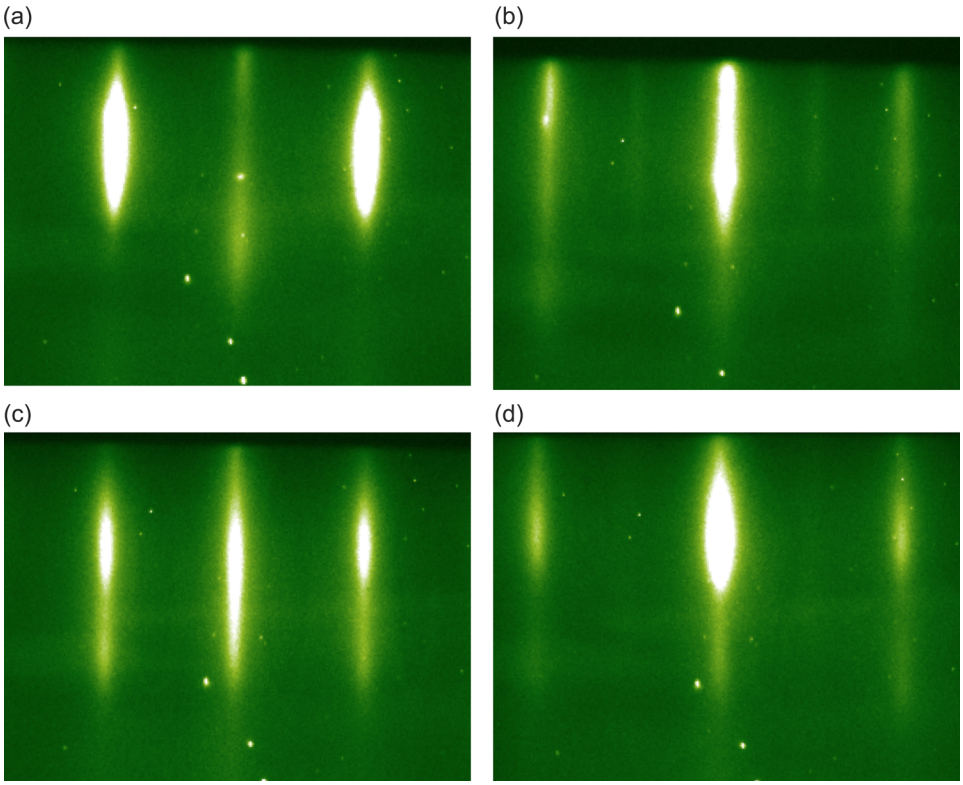

FIG. 3. (Color online) RHEED images of the 5 unit-cell-thick $SrTiO_3$ along the [100] (a) and [110] (b) azimuth of the (001) $SrTiO_3$ surface showing that the thin $SrTiO_3$ film is smooth. RHEED images of the 10 nm thick $LaAlO_3$ film after growth viewed along the [100] (c) and [110] (d) azimuth indicate that the 10 nm thick $LaAlO_3$ film is smooth and single crystalline. These RHEED images are from the growth of the same film grown with the parameters shown in Figs. 1 and 2.

the incident beam along the [100] and [110] azimuth of the (001) $SrTiO_3$ surface are shown in Figs. 3(a) and 3(b), respectively. RHEED patterns of the 10 nm thick $LaAlO_3$ film after growth are shown in Figs. 3(c) and 3(d), along the [100] and [110] azimuth of the (001) $LaAlO_3$ surface, respectively. The streaky patterns show that the surface of both the 5 unit-cell-thick $SrTiO_3$ and 10 nm thick $LaAlO_3$ grown on it are smooth. No extra spots were detected from RHEED patterns during or after the growth, indicating that the film is epitaxial and single phase.

XRD was measured with both Rigaku SmartLab and PANalytical X'Pert diffractometers, utilizing Cu $K_{\alpha 1}$ radiation. Figure 4(a) shows the θ-2θ measurement of the same heterostructure characterized in Figs. 1–3. The presence of only 00ℓ reflections in combination with the RHEED [Figs. 3(c) and 3(d)] from the 10 nm thick $LaAlO_3$ layer indicates that the $LaAlO_3$ film is single crystalline and phase-pure. Clear Kiessig fringes[36] can be seen in the θ-2θ scan, signifying that the interfaces of the heterostructure are smooth.

The rocking curve in ω of the $LaAlO_3$ 002 peak was measured to assess the crystalline perfection of the 10 nm thick $LaAlO_3$ film. The result is shown in Fig. 4(b). The rocking curve has a full width at half maximum (FWHM) value of 0.02°, which is the narrowest FWHM ever reported for $LaAlO_3$ films on silicon and indicates that the 10 nm thick $LaAlO_3$ film possesses a high degree of crystalline perfection. The in-plane orientation relationship between the $LaAlO_3$ film and the silicon substrate was confirmed with a ϕ scan: (001) $LaAlO_3$ || (001) Si and [110] $LaAlO_3$ || [100] Si, as is shown in Fig. 4(c). The ϕ scan of the 10 nm thick $LaAlO_3$ film has a FWHM of ~1°, which means that the in-plane mosaic spread is relatively large. This might be inherited from the in-plane mosaic spread of the $SrTiO_3$ buffer layer (The narrowest FWHM in ϕ of $SrTiO_3$ grown on silicon that has been reported is 0.5°.[37] Indeed improving in-plane registry between $SrTiO_3$ and silicon remains a major unsolved challenge.) and is consistent with the broad feature of the $LaAlO_3$ 103 peak from the reciprocal space mapping (RSM), as is shown in Fig. 4(d). The RSM of the Si 115 peak is shown in Fig. 4(d) for comparison.

Rocking curves of several $LaAlO_3$ single crystals (measured on commercial substrates) contain multiple peaks due to the existence of twins,[1] as is shown in Fig. 5(a). Compared to commercial (001) $LaAlO_3$ single crystal substrates, our 10 nm thick $LaAlO_3$ film on silicon shows a comparable rocking curve FWHM. Next, we compare the rocking curve FWHM in ω of our best 10 nm thick $LaAlO_3$ film on silicon with previous results for such films from the literature. Figure 5(b) shows this comparison and signifies that we have enhanced the crystalline quality of the $LaAlO_3$ film on $SrTiO_3$-buffered silicon by almost an order of magnitude. We also include the rocking curve FWHM of a thick $LaAlO_3$ film grown on a (001) $SrTiO_3$ single crystal substrate[38] for comparison.

XRD was used to check the strain state of the resulting $LaAlO_3$ film on silicon. If $LaAlO_3$ was commensurately strained to the underlying silicon substrate, it should have an out-of-plane lattice spacing given approximately by 3.753 Å, assuming isotropic elasticity and the epitaxial film to have

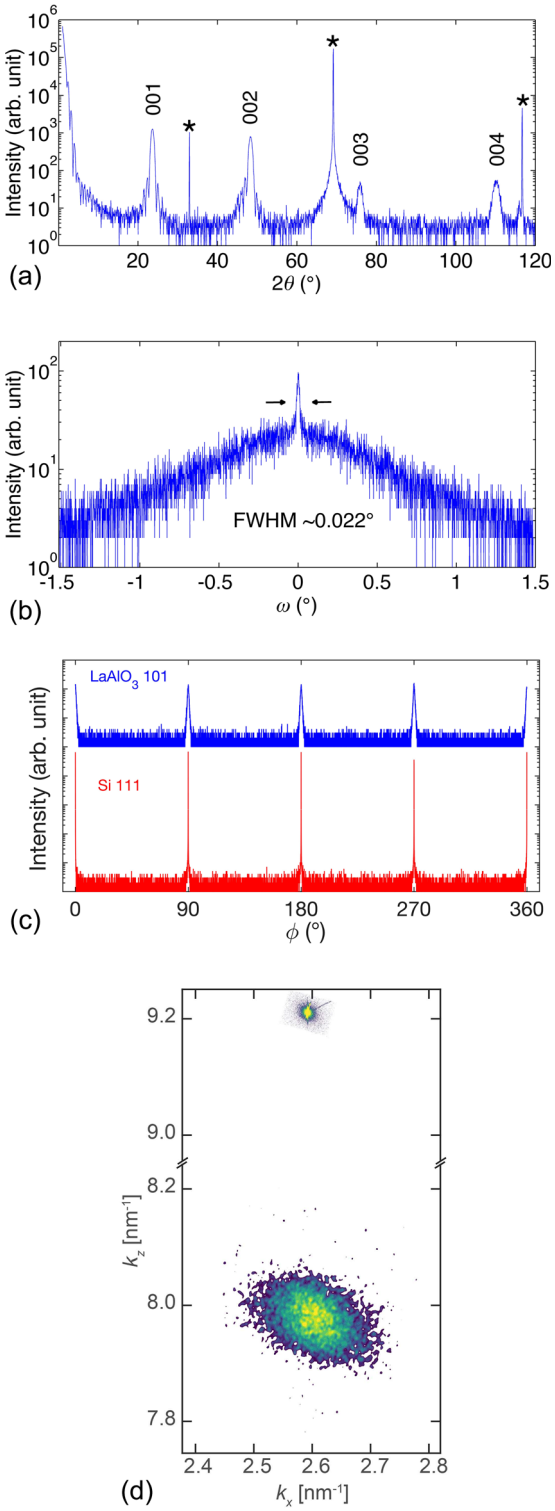

FIG. 4. (Color online) XRD measurements of the same heterostructure (10 nm $LaAlO_3$ on the 5 unit-cell-thick $SrTiO_3$ buffer layer on silicon that was characterized in Figs. 1–3). θ-2θ scan (a) shows only 00ℓ reflections of $LaAlO_3$. This, in conjunction with the RHEED, indicates that the $LaAlO_3$ film grew epitaxially on the 5 unit-cell-thick $SrTiO_3$ on silicon. The small hump near $2\theta = 46°$ comes from the 5 unit-cell-thick $SrTiO_3$. Rocking curve in ω (b) of the $LaAlO_3$ 002 peak shows a single peak with a FWHM of 0.02°. ϕ scan (c) shows that the in-plane epitaxial relationship between the 10 nm thick (001) $LaAlO_3$ and the (001) Si substrate is cube-on-cube with a 45° in-plane rotation. Plots of the $LaAlO_3$ 101 family of peaks and the Si 111 family of peaks are offset for clarity. RSMs of the $LaAlO_3$ 103 peak and the Si 115 peak (d) indicate a relatively large in-plane broadening for the 10 nm thick $LaAlO_3$ film.

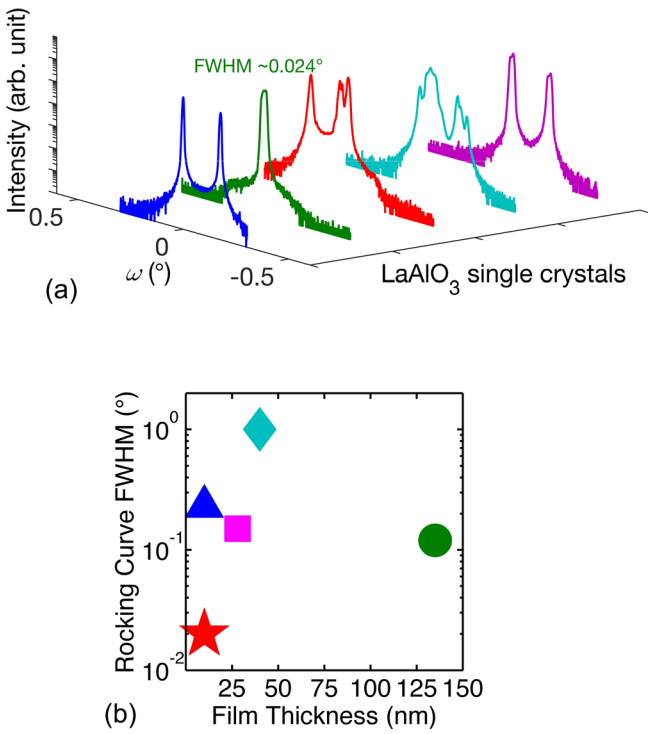

FIG. 5. (Color online) FWHM of the rocking curves of the $LaAlO_3$ 002 peak of several commercial (001) $LaAlO_3$ single crystals (a) shows multiple peaks due to the twinning of the $LaAlO_3$ single crystal. The rocking curve FWHM of the 10 nm thick $LaAlO_3$ on the 5 unit-cell-thick $SrTiO_3$ on silicon is comparable to the narrowest FWHM value of ~0.024° for $LaAlO_3$ single crystals. A comparison of rocking curve FWHM of our film with the narrowest values reported in the literature (b) shows that we have narrowed the FWHM of the $LaAlO_3$ layer on silicon by almost an order of magnitude. The diamond-, square-, and triangle-shaped data points are from Refs. 22–24, respectively. The horizontal axis indicates the thickness of the $LaAlO_3$ films grown on silicon. The circular data point is from a $LaAlO_3$ film grown on an $SrTiO_3$ single crystal substrate from Ref. 38.

the same Poisson ratio ($\upsilon = 0.26$) as bulk $LaAlO_3$.[39] The measured out-of-plane lattice parameter of the $LaAlO_3$ film, derived from the θ-2θ scan using a Nelson-Riley fit,[40] is 3.761 ± 0.003 Å, indicating that the film is not commensurately strained. Another possibility is that the 1.3% misfit strain between the $LaAlO_3$ film and the silicon substrate relaxed fully during growth. The out-of-plane lattice spacing in this case, assuming that the only strain on the $LaAlO_3$ film arises due to the relatively large difference in the thermal expansion coefficients of silicon (averaging 3.5×10^{-6} K^{-1} between room temperature and 520 °C)[41] and $LaAlO_3$ (averaging 8.5×10^{-6} K^{-1} between room temperature and 520 °C),[42] is calculated as follows: If the 10 nm thick $LaAlO_3$ film were fully relaxed at 580 °C, its pseudocubic lattice parameter ($a^{LaAlO_3}_{in-plane,\ 580\,°C}$) would be equal to that of bulk $LaAlO_3$, which is approximately 3.807 Å at 580 °C.[42] Assuming that on cooling the $LaAlO_3$ film is fully clamped to the underlying silicon substrate, we have[43]

$$a^{10\,nm\,LaAlO_3}_{in-plane,\ 25\,°C} - a^{10\,nm\,LaAlO_3}_{in-plane,\ 580\,°C} = \frac{a^{silicon}_{in-plane,\ 25\,°C} - a^{silicon}_{in-plane,\ 580\,°C}}{\sqrt{2}}, \quad (1)$$

where $a^{silicon}_{in-plane,\ 25\,°C}/\sqrt{2} = 3.84$ Å and $a^{silicon}_{in-plane,\ 580\,°C}/\sqrt{2} = 3.848$ Å. The out-of-plane lattice parameter of the 10 nm $LaAlO_3$ film under the above assumptions and assuming isotropic elasticity can be calculated via

$$a^{10\,nm\,LaAlO_3}_{out-of-plane,\ 25\,°C} = \frac{2\upsilon}{\upsilon - 1} a^{10\,nm\,LaAlO_3}_{in-plane,\ 25\,°C} + \frac{1+\upsilon}{1-\upsilon} a^{LaAlO_3}_{0,\ 25\,°C}, \quad (2)$$

where $\upsilon = 0.26$ is the Poisson ratio of $LaAlO_3$[39] and $a^{LaAlO_3}_{0,\ 25\,°C}$ is 3.790 Å. From Eq. (2), $a^{10\,nm\,LaAlO_3}_{out-of-plane,\ 25\,°C}$ is calculated to be 3.782 Å, which is larger than the measured value of 3.761 ± 0.003 Å. This means that the 10 nm thick $LaAlO_3$ film is not fully relaxed. Further calculations based on the in-plane lattice constant for the $LaAlO_3$ film—3.778 ± 0.004 Å—obtained from the RSM of the $LaAlO_3$ 103 peak [Fig. 4(d)] show that the 10 nm thick $LaAlO_3$ film is 90% relaxed.

The surface roughness of the as-grown 10 nm thick $LaAlO_3$ film on silicon was evaluated by AFM utilizing an Asylum Research MFP-3D in the tapping mode. Figures 6(a) and 6(b) show the surface height scan and the three dimensional height scan of the same sample characterized in Figs. 1–5, respectively. The root mean square of the surface roughness is ~1.3 Å, which is comparable to the best $LaAlO_3$-on-silicon films reported in the literature.[22] The smooth surface is beneficial for the integration of overlying functional oxides including the synthesis of superlattices.

The interface abruptness and microstructure of the same heterostructure characterized in Figs. 1–6 were investigated

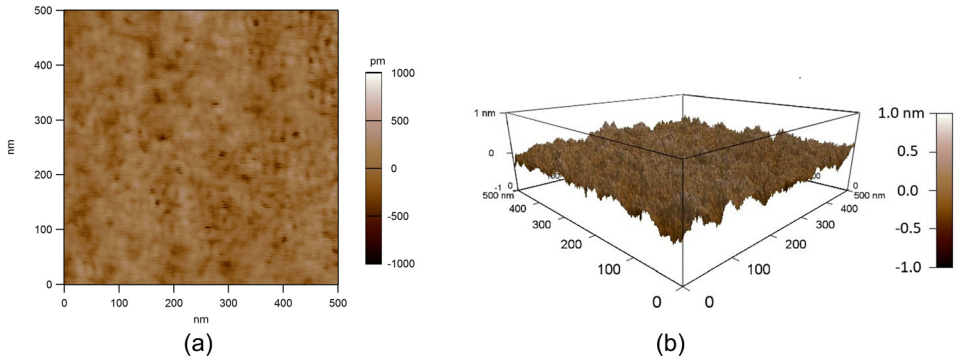

FIG. 6. (Color online) AFM images of the same 10 nm thick $LaAlO_3$ film grown on the 5 unit-cell-thick $SrTiO_3$ on silicon that was characterized in Figs. 1–5. The surface height scan (a) as well as the three dimensional image (b) reveals a relatively smooth surface of the as-grown 10 nm thick $LaAlO_3$ film on silicon.

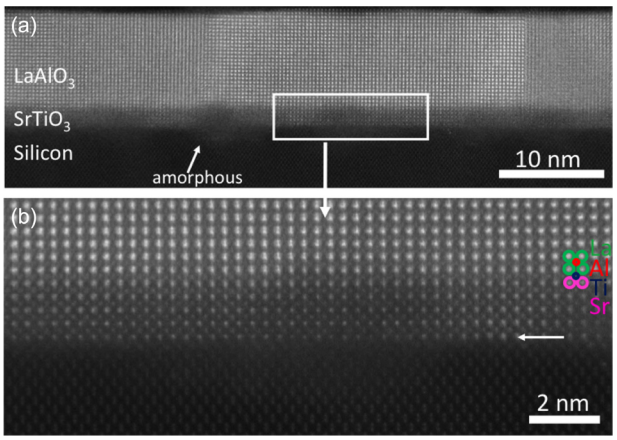

FIG. 7. (Color online) HAADF STEM image (a) of the same 10 nm thick $LaAlO_3$ on a 5 unit-cell-thick $SrTiO_3$ buffer layer on silicon that was characterized in Figs. 1–6. It is clear from (a) that the $LaAlO_3/SrTiO_3$ interface is relatively sharp. Most of the $SrTiO_3$/Si interface is crystalline, with small portion of the interface being amorphous. An expanded view (b) of a section with the crystalline $SrTiO_3$/Si interface (indicated by the arrow) is shown below. A schematic drawing is overlaid to indicate the atom configuration of $LaAlO_3$ and $SrTiO_3$.

by aberration-corrected STEM. High-angle annular dark field (HAADF) images were taken at 300 kV with a 21.4 mrad probe-forming semiangle on an FEI-Titan Themis. Figure 7(a) reveals a clear interface between the $LaAlO_3$ and $SrTiO_3$ layers. The atomic configuration of the interface is shown in the inset on top of the STEM image in the magnified image of Fig. 7(b). Most of the $SrTiO_3$/Si interface is crystalline and nearly free of an amorphous SiO_2 layer, but amorphous layers exist in small sections of the $SrTiO_3$/Si interface. The preservation of this relatively high crystalline interface is attributed to the controlled growth of the 5 unit-cell-thick $SrTiO_3$ layer[30] as well as the careful transition between the thin $SrTiO_3$ buffer layer and the $LaAlO_3$ layer on top of it.

IV. SUMMARY AND CONCLUSIONS

Using MBE, we have grown $LaAlO_3$ films with high crystalline quality on $SrTiO_3$-buffered silicon. A $LaAlO_3$ film with a rocking curve FWHM of 0.02° was achieved, which is the narrowest for $LaAlO_3$ films on silicon and is comparable to single-crystal $LaAlO_3$ substrates. The surface of the film is smooth with a root mean square roughness of ∼1.3 Å by AFM. STEM reveals both the $LaAlO_3/SrTiO_3$ and the $SrTiO_3$/Si interfaces to be sharp. The improved perfection of $LaAlO_3$ on silicon paves the way for utilizing $LaAlO_3$ as a template layer for growing closely lattice matched functional oxides with high crystalline quality on top of silicon, thus enabling the novel phenomena observed in oxide heterostructures to be integrated with the backbone of semiconductor technology.

ACKNOWLEDGMENTS

The authors gratefully acknowledge stimulating discussions with Kiyoung Lee and Eunsun Kim and the support from a GRO 'functional oxides' project from the Samsung Advanced Institute of Technology. Zhen Chen was supported by the National Science Foundation [Platform for the Accelerated Realization, Analysis, and Discovery of Interface Materials (PARADIM)] under the Cooperative Agreement No. DMR-1539918. This work made use from the Cornell Center for Materials Research (CCMR) Shared Facilities, which are supported through the NSF MRSEC program (DMR-1719875). Substrate preparation was performed in part at the Cornell NanoScale Facility, a member of the National Nanotechnology Coordinated Infrastructure (NNCI), which is supported by the NSF (Grant No. ECCS-15420819).

[1]S. Geller and V. B. Bala, Acta Crystallogr. **9**, 1019 (1956).
[2]K. J. Hubbard and D. G. Schlom, J. Mater. Res. **11**, 2757 (1996).
[3]D. G. Schlom and J. H. Haeni, MRS Bull. **27**, 198 (2002).
[4]R. W. Simon, C. E. Platt, A. E. Lee, G. S. Lee, K. P. Daly, M. S. Wire, J. A. Luine, and M. Urbanik, Appl. Phys. Lett. **53**, 2677 (1988).
[5]R. A. Rao, Q. Gan, C. B. Eom, R. J. Cava, Y. Suzuki, J. J. Krajewski, S. C. Gausepohl, and M. Lee, Appl. Phys. Lett. **70**, 3035 (1997).
[6]S. G. Ghonge, E. Goo, R. Ramesh, T. Sands, and V. G. Keramidas, Appl. Phys. Lett. **63**, 1628 (1993).
[7]K. M. Satyalakshmi, R. M. Mallya, K. V. Ramanathan, X. D. Wu, B. Brainard, D. C. Gautier, N. Y. Vasanthacharya, and M. S. Hegde, Appl. Phys. Lett. **62**, 1233 (1993).
[8]R. J. Zeches *et al.*, Science **326**, 977 (2009).
[9]S. Jin, T. H. Tiefel, M. McCormack, R. A. Fastnacht, R. Ramesh, and L. H. Chen, Science **264**, 413 (1994).
[10]M. A. Novojilov, O. Yu. Gorbenko, I. E. Graboy, A. R. Kaul, H. W. Zandbergen, N. A. Babushkina, and L. M. Belova, Appl. Phys. Lett. **76**, 2041 (2000).
[11]M. Kamei, T. Miyagi, and T. Ishigaki, Chem. Phys. Lett. **407**, 209 (2005).
[12]A. T. Findikoglu, Q. X. Jia, X. D. Wu, G. J. Chen, T. Venkatesan, and D. W. Reagor, Appl. Phys. Lett. **68**, 1651 (1996).
[13]L. A. Knauss, J. M. Pond, J. S. Horwitz, D. B. Chrisey, C. H. Mueller, and R. Treece, Appl. Phys. Lett. **69**, 25 (1996).
[14]K. S. Takahashi, M. Kawasaki, and Y. Tokura, Appl. Phys. Lett. **79**, 1324 (2001).
[15]G. Malandrino, A. Frassica, and I. L. Fragalà, Chem. Vap. Deposition **3**, 306 (1997).
[16]X. B. Lu, Z. G. Liu, X. Zhang, R. Huang, H. W. Zhou, X. P. Wang, and B.-Y. Nguyen, J. Phys. D: Appl. Phys. **36**, 3047 (2003).
[17]E. Sader, H. Schmidt, K. Hradil, and W. Wersing, Supercond. Sci. Technol. **4**, 371 (1991).
[18]K. Kukli *et al.*, Chem. Vap. Deposition **12**, 158 (2006).
[19]O. K. Dmitri, D. G. Schlom, H. Li, and S. Stemmer, Jpn. J. Appl. Phys., Part 2 **44**, L617 (2005).
[20]T. L. Chu, M. H. Francombe, G. A. Gruber, J. J. Oberly, and R. L. Tallman, Report No. AFCRL-65-574, Westinghouse Research Laboratories, Pittsburgh, 1965).
[21]C. A. Billman, R. A. McKee, F. J. Walker, M. F. Chisholm, J. Lettieri, and D. G. Schlom, *12th International Symposium on Integrated Ferroelectrics (ISIF 2000)*, Aachen, Germany (2000).
[22]W. F. Xiang, H. B. Lu, Z. H. Chen, X. B. Lu, M. He, H. Tian, Y. L. Zhou, C. R. Li, and X. L. Ma, J. Cryst. Growth **271**, 165 (2004).
[23]J. W. Reiner, A. Posadas, M. Wang, T. P. Ma, and C. H. Ahn, Microelectron. Eng. **85**, 36 (2008).
[24]T. Q. Ngo, A. Posadas, M. D. McDaniel, D. A. Ferrer, J. Bruley, C. Breslin, A. A. Demkov, and J. G. Ekerdt, J. Cryst. Growth **363**, 150 (2013).
[25]C. G. Bischak, C. L. Hetherington, Z. Wang, J. T. Precht, D. M. Kaz, D. G. Schlom, and N. S. Ginsberg, Nano Lett. **15**, 3383 (2015).
[26]C. D. Theis and D. G. Schlom, J. Vac. Sci. Technol., A **14**, 2677 (1996).
[27]J. Lettieri, J. H. Haeni, and D. G. Schlom, J. Vac. Sci. Technol., A **20**, 1332 (2002).
[28]H. Li *et al.*, J. Appl. Phys. **93**, 4521 (2003).
[29]M. P. Warusawithana *et al.*, Science **324**, 367 (2009).
[30]Z. Wang *et al.*, "Enhancement of crystalline quality of $SrTiO_3$ on silicon," APL Mater. (submitted).
[31]M. P. Warusawithana *et al.*, Nat. Commun. **4**, 2351 (2013).

[32]S.-H. Baek and C. B. Eom, Acta Mater. **61**, 2734 (2013).
[33]W.-F. Xiang, H.-B. Lu, Z.-H. Chen, M. He, and Y.-L. Zhou, Chin. Phys. Lett. **22**, 1515 (2005).
[34]C. S. Hellberg, K. E. Andersen, H. Li, P. J. Ryan, and J. C. Woicik, Phys. Rev. Lett. **108**, 166101 (2012).
[35]L. F. Kourkoutis, C. S. Hellberg, V. Vaithyanathan, H. Li, M. K. Parker, K. E. Anderson, D. G. Schlom, and D. A. Muller, Phys. Rev. Lett. **100**, 049901 (2008).
[36]H. Kiessig, Ann. Phys. **402**, 769 (1931).
[37]J. Lettieri, *Critical Issues of Complex, Epitaxial Oxide Growth and Integration with Silicon by Molecular Beam Epitaxy* (Pennsylvania State University, University Park, 2002), p. 106.
[38]M. Nieminen, T. Sajavaara, E. Rauhala, M. Putkonen, and L. Niinistö, J. Mater. Chem. **11**, 2340 (2001).
[39]M. A. Carpenter, T. W. Darling, J. D. Bass, D. L. Lakshtanov, S. V. Sinogeikin, and S. D. Jacobsen, *American Geophysical Union Fall Meeting* (2006).
[40]J. B. Nelson and D. P. Riley, Proc. Phys. Soc. **57**, 160 (1945).
[41]Y. S. Touloukian, R. Kirby, E. Taylor, and T. Lee, *Thermal Expansion: Nonmetallic Solids, Volume 13 of Thermophysical Properties of Matter* (Plenum, New York, 1977), p. 154.
[42]B. C. Chakoumakos, D. G. Schlom, M. Urbanik, and J. Luine, J. Appl. Phys. **83**, 1979 (1998).
[43]L. Zhang and R. Engel-Herbert, Phys. Status Solidi RRL **8**, 917 (2014).